# Closure for the Ornstein-Zernike equation with pressure and free energy consistency

Tsogbayar Tsednee and Tyler Luchko

Phys. Rev. E **99**, 032130 — Published 25 March 2019

DOI: 10.1103/PhysRevE.99.032130

# A closure for the Ornstein-Zernike equation with pressure and free energy consistency

Tsogbayar Tsednee and Tyler Luchko*
*Department of Physics and Astronomy, California State University Northridge, 18111 Nordhoff Street, Northridge, CA 91333, USA*
(Dated: March 8, 2019)

The Ornstein-Zernike (OZ) integral equation theory is a powerful approach to simple liquids due to its low computational cost and the fact that, when combined with an appropriate closure equation, the theory is thermodynamically complete. However, approximate closures proposed to date exhibit pressure or free energy inconsistencies that produce inaccurate or ambiguous results, limiting the usefulness of the Ornstein-Zernike approach. To address this problem, we combine methods to enforce both pressure and free energy consistency to create a new closure approximation and test it for a single-component Lennard-Jones fluid. The closure is a simple power series in the direct and total correlation functions, for which we have derived analytical formulas for the excess Helmholtz free energy and chemical potential. These expressions contain a partial molar volume-like term, similar to excess chemical potential correction terms recently developed. Using our new bridge approximation, we have calculated the pressure, Helmholtz free energy, and chemical potential for the Lennard-Jones fluid using the Kirkwood charging, thermodynamic integration techniques, and analytic expressions. These results are compared with those from the hypernetted chain equation and the Verlet-modified closure against Monte Carlo and equations-of-state data for reduced densities of $\rho^* < 1$ and temperatures of $T^* = 1.5$, 2.74, and 5. Our new closure shows consistency among all thermodynamic paths, except for one expression of the Gibbs-Duhem relation, whereas the hypernetted chain equation and Verlet-modified closure only exhibit consistency between a few relations. Accuracy of the new closure is comparable to Verlet-modified closure and a significant improvement to results obtained from the hypernetted chain equation.

## I. INTRODUCTION

Integral equation and classical density functional theories of the statistical mechanics of liquids are frequently used in the study of biological, condensed matter and plasma systems due to their low computational cost and the physical insights they provide. Over the years, fundamental theories, such as the Ornstein-Zernike (OZ) equation [1] and classical density functional theory (CDFT) [2], have been developed to deal with complex solutes and molecular solvents; e.g., reference interaction site model (RISM) theories [3–7], molecular OZ[8, 9], and molecular CDFT [10]. Common to all these theories is the requirement of a closure relation. Unfortunately, approximations to the closure equation have invariably produce inconsistent state variables that depend on the physical or mathematical path taken – i.e., thermodynamic inconsistencies – that should not exist. Importantly, quantitatively different pressures or free energies are calculated when different thermodynamic routes are employed. Such inconsistencies limit physical insights and affect the accuracy of the theory. Despite an immense amount of work on the subject, no closure approximation has been developed that incorporates both free energy and pressure consistency.

Pressure consistency may been enforced by introducing free parameters into a closure approximation, which are adjusted to ensure density derivatives of the pressure calculated from the virial and compressibility paths agree. Many closure approximations of this type have been developed and improved the accuracy of calculated pressures [11–19]. However, these closures have failed to provide path independent free energies, limiting their usefulness.

Free energy consistency can be guaranteed by satisfying conditions derived by Kast [20], which only a small number of closely related closures have been shown to satisfy [7, 21, 22]. However, these closures do not display pressure consistency and both pressure and free energy estimates are inaccurate [23]. In fact, to compensate for the large errors, a number of partial molar volume (PMV) corrections have been developed that are applied to just the chemical potential [24–27].

In this work, we show how these two approaches can be combined by proposing a simple closure approximation compatible with both. We show that this closure not only satisfies both pressure and free energy consistency relations but also internal energy-pressure, free energy-pressure, and Gibbs-Duhem consistency. Furthermore, we derived analytic, closed-form formulas for both the chemical potential and Helmholtz free energy. The formula for the chemical potential is functionally similar to that of the hypernetted chain equation (HNC) [21] with the Universal Correction (UC) [24] applied. We then apply this closure to a simple Lennard-Jones fluid at densities $\rho\sigma^3 = 0.1$ to 1.1, and temperatures $T^* = 1.5, 2.74$ and 5 in reduced units and compare it to the HNC and Verlet-modified (VM) [28], which exhibit free energy and pressure consistency respectively. Several consistency relations are checked for all three approximations and results for the excess free

* tluchko@csun.edu

energy and excess chemical potential are compared with available simulation and equation of state data [29–31].

The paper is organized as follows. In Section II we discuss theoretical foundations for developing a closure with thermodynamic consistency and introduce our closure approximation. We also provide an overview of the consistency tests we will use. Numerical procedures used to calculate thermodynamic quantities are described in Section III. In Section IV we present our results and in Section V we discuss the implications for thermodynamic consistency and the relationship to PMV corrections. This is followed by concluding remarks.

## II. THEORY

### Ornstein-Zernike equation

Many excellent descriptions of the OZ equation can be found in the literature such as [32, 33]. Briefly, the OZ equation divides the contributions to equilibrium liquid structure into direct and indirect contributions. For a homogeneous, single component system at temperature $T$ and number density $\rho$, it may be written in the form

$$h(r) = c(r) + \rho \int c(|\boldsymbol{r} - \boldsymbol{r}'|)h(\boldsymbol{r}')d\boldsymbol{r}' \tag{1}$$

where $h(r)$ and $c(r)$ are the total and the direct correlation functions, respectively. With these functions, one can define the indirect correlation, $\gamma \equiv h(r) - c(r)$, and radial distribution functions, $g(r) = h(r) + 1$.

To solve Eq. (1), one needs a second equation, called a *closure relation*, that relates the correlation functions to a spherically symmetric pair potential $u(r)$ between the liquid particles. This closure equation is defined as

$$h(r) = \exp[-\beta u(r) + \gamma(r) + B(r)] - 1, \tag{2}$$

where $B(r)$ is the bridge function, $\beta = 1/k_{\mathrm{B}}T$, and $k_{\mathrm{B}}$ is the Boltzmann constant. $B(r)$ can be expressed as a power series in $\rho$ of irreducible diagrams [34] but, in practice, is approximated as some combination of $u\,(r)$, $h\,(r)$, and $c\,(r)$. By solving Eqs. (1) and (2) self-consistently, both correlation functions may be obtained. Commonly used closures include the HNC,

$$B_{\mathrm{HNC}}(r) = 0, \tag{3}$$

and a VM approximation [28],

$$B_{\mathrm{VM}}(r) = -\frac{1}{2}\frac{\phi\gamma_a^2}{1 + \alpha\gamma_a}, \tag{4}$$

where $\phi$ and $\alpha$ are free parameters to be optimized. Here $\gamma_a \equiv \gamma - \beta u_a$ and $u_a(r)$ is the attractive part of the pair potential [35].

### Thermodynamic consistency and the bridge function

As a closed form expression for the bridge function is not known, one must attempt to build an approximate bridge function, $B(r)$, either theoretically or empirically. For the former approach, one needs to compute a series expansion for $B(r)$ in powers of the density, in which each term may represent the sum of diagrams computed in terms of the multidimensional integrals, and so cannot be completely utilized in practice [34, 36, 37].

The empirical approach is technically easier. However, when constructing $B(r)$, one should take care to preserve the thermodynamic consistency, which is the property that state variables do not depend on the path taken in the physical or mathematical sense. There are several types of thermodynamic consistency conditions, for example [38–40]: virial and compressibility pressure,

$$p^v = p^c, \tag{5}$$

internal energy and pressure,

$$\rho^2 \left(\frac{\partial \beta E/N}{\partial \rho}\right)_T = -T\left(\frac{\partial \beta p}{\partial T}\right)_\rho, \tag{6}$$

pressure and free energy,

$$\beta\mu^e = \frac{\beta A^e}{N} + \frac{\beta p}{\rho} - 1, \tag{7}$$

and Gibbs-Duhem

$$\left(\frac{d\mu}{dp}\right)_T = \frac{1}{\rho}. \tag{8}$$

These conditions can either be directly tested for or explicitly enforced; e.g., through the introduction free parameters in the closure relation that can be tuned. In this work, we enforce Eq. (5) and test the other three relations.

In addition, we require path independence for the chemical potential and Helmholtz free energy. For example, the results of the Kirkwood charging formulas for chemical potential and free energy, Eqs. (C1) and (B1), should not depend on how the coupling parameter is included. To handle this path-dependence issue, Kast [20] has shown that path independence is implied if the variational parameter

$$q = \frac{\frac{\partial B}{\partial \gamma} - \frac{\partial B}{\partial c} + 1}{\frac{\partial B}{\partial u} - \beta} \tag{9}$$

is independent of the spatial coordinates and $\lambda$ (see also Appendix B). Therefore, any function $B(\gamma - \beta u)$, $B(c + \beta u)$, $B(h, \gamma - \beta u)$, $B(h, c + \beta u)$ and $B(h)$ has guaranteed path independence in RISM theory and, therefore, OZ theory. Importantly, renormalized bridge functions, where only the long-range or short-range part of the potential is used, do not satisfy this condition. Nor do functions that are a function of $\gamma$, $B\,(\gamma)$. Such bridge functions may be path-independent but this is difficult to prove and must be done on an individual basis.

**A free energy and pressure path-independent closure**

In this work we employ virial and compressibility pressure consistency, commonly known as "pressure consistency", and free energy consistency. As we are not aware of a bridge approximation that has both properties, we propose a new approximation which satisfies the Kast conditions and has free parameters, $a$ and $b$, to enforce pressure consistency,

$$B(r) = ac(r) + \sum_i b_i h^i(r). \quad i = 1, 2, 3, \ldots \tag{10}$$

Although this proposed equation explicitly includes the direct correlation function, it satisfies the requirements for path-independence since Eq. (9) is constant and independent of spatial coordinates and coupling parameters. Details are given in Appendix B. For simplicity, in the numerical part of this work we employ only the first order expansion of the proposed bridge function,

$$B = ac(r) + b_1 h(r). \tag{11}$$

In order to simplify the computational work required, it is advantageous to have an analytical, closed-form expression to evaluate the excess free energy or chemical potential. Using the Kirkwood charging formula, we can obtain an analytic formula for evaluation of the excess Helmholtz free energy (see Appendix C):

$$\begin{aligned}\frac{\beta A^e}{N} = \frac{\beta A^{\mathrm{HNC}}}{N} &+ \frac{\rho}{2}\int d\boldsymbol{r} g B \\ &- \frac{a}{16\pi^3}\int d\boldsymbol{k}\left[\hat{h} - \frac{1}{\rho}\ln\left|1+\rho\hat{h}\right|\right] \\ &- \frac{\rho}{2}\int \sum_i \frac{b_i}{i+1} h^{i+1} d\mathbf{r}.\end{aligned} \tag{12}$$

Here, $\frac{\beta A^{\mathrm{HNC}}}{N}$ is the excess Helmholtz free energy expression for the HNC closure is given by [34, 41],

$$\begin{aligned}\frac{\beta A^{\mathrm{HNC}}}{N} = &\frac{\rho}{2}\int d\boldsymbol{r}\Big(\frac{1}{2}h^2 - c\Big) \\ &+ \frac{1}{2}\frac{1}{8\pi^3}\int d\boldsymbol{k}\Big[\hat{c} + \frac{1}{\rho}\ln|1-\rho\hat{c}|\Big].\end{aligned} \tag{13}$$

Using similar approach (see Appendix C) we can obtain a semi-analytical expression for the VM closure

$$\begin{aligned}\frac{\beta A^e}{N} = \frac{\beta A^{\mathrm{HNC}}}{N} &+ \frac{\rho}{2}\int d\boldsymbol{r} g B + \frac{\rho}{4}\frac{1}{8\pi^3}\int d\boldsymbol{k}\hat{h} \\ &\times \int_0^1 d\nu \left(\frac{\phi\left(\rho\nu^2\hat{h}^2/\left(1+\rho\nu\hat{h}\right)\right)^2}{1+\alpha\rho\nu^2\hat{h}^2/\left(1+\rho\nu\hat{h}\right)}\right).\end{aligned} \tag{14}$$

where numerical integration over a coupling parameter, $\nu$, is still required.

For excess chemical potential we have derived a formula with the proposed bridge function (see Appendices B and C):

$$\begin{aligned}\beta\mu^e = \beta\mu^{\mathrm{HNC}} &+ \rho\int d\boldsymbol{r} g B \\ &- \rho\int d\boldsymbol{r}\left[\frac{1}{2}ahc + \left(\sum_{i=1}\frac{b_i}{i+1}h^{i+1}\right)\right],\end{aligned} \tag{15}$$

where $\beta\mu^{\mathrm{HNC}}$ is the HNC-type expression for the excess chemical potential with appropriate bridge function $B(r)$ [34, 41],

$$\beta\mu^{\mathrm{HNC}} = \rho\int d\boldsymbol{r}\Big(\frac{1}{2}h^2 - c - \frac{1}{2}hc\Big). \tag{16}$$

The VM closure has no known closed-form, analytic expression for the excess chemical potential. Instead, we will employ a commonly used approximate closed expression [42–46],

$$\beta\mu^e \approx \beta\mu^{\mathrm{HNC}} + \rho\int d\boldsymbol{r}\Big(B + \frac{2h}{3}B\Big). \tag{17}$$

With Eqs. (12) to (17) the excess Helmholtz free energy and chemical potential can be computed using only a single state at the given temperature and density. As one would expect, setting $B = 0$ in the derived expressions for the HFE and chemical potential leads directly to expressions in the HNC approximation, Eq. (13). We note that for the excess free energy, expressions similar to formula Eq. (14) have been given by Kiselyov and Martynov [42], but for other closure approximations.

**Evaluating thermodynamic consistency**

To check if a closure approximation satisfies Eqs. (5)-(7), we must compute pressure, internal energy, free energy and chemical potential using different paths. These different paths may involve numerical integration and differentiation or different analytic expressions for the same quantity.

*Virial and compressibility pressure*

Pressure consistency is most commonly calculated along the viral and compressibility paths, Eq. (5). The pressure from the virial equation of state, $p^v$, [32] is computed as,

$$\frac{\beta p^v}{\rho} = 1 - \frac{\rho}{6}\int d\boldsymbol{r} r\frac{\partial\beta u(r)}{\partial r} g(r), \tag{18}$$

where $\beta = 1/k_b T$, $k_b$ is Boltzmann's constant and $T$ is temperature. The isothermal compressibility, $\chi_T$, is computed through the compressibility route [32],

$$\beta(\rho\chi_T)^{-1} = \beta\left(\frac{\partial p^c}{\partial\rho}\right)_T = 1 - \rho\int c(r)d\boldsymbol{r}, \tag{19}$$

where $p^c$ is the pressure from the compressibility route and the pressure can be computed as

$$\frac{\beta p^c}{\rho} = \frac{\beta}{\rho}\int_0^\rho d\rho' \rho'^{-1}\chi_T^{-1}. \tag{20}$$

*Internal energy and pressure*

To check the consistency of the internal energy and pressure, Eq. (6), the temperature derivatives of the internal energy and pressure are required. The internal energy may be directly computed as [32]

$$\begin{aligned} E &= E^i + E^e \\ &= \frac{3}{2}k_bT + \frac{\rho}{2}\int g\left(\mathbf{r}\right)u\left(\mathbf{r}\right)\mathrm{d}\mathbf{r} \end{aligned} \tag{21}$$

where $E^e$ is the excess internal energy and $E^i$ is the internal energy of the ideal gas. Temperature and density derivatives of Eq. (20) and Eq. (21) are straightforward to compute.

*Pressure and free energy*

Pressure and free energy consistency, Eq.(7), may be tested by comparing chemical potentials calculated along different paths. Analytical expressions for chemical potential, Eqs. (15) and (16), are guaranteed to be path independent. In addition, the virial and compressibility pressure equations may be combined with the Helmholtz free energy using Eq. (7). The excess Helmholtz free energy may be computed from the Kirkwood charging formula, such as the analytic and semi-analytic expressions already presented, Eqs. (12), (13), and (14), or by integrating along the density path [30, 47]

$$\frac{\beta A^e}{N} = \int_0^\rho d\rho' \frac{1}{\rho'}\Big(\frac{\beta p}{\rho'} - 1\Big). \tag{22}$$

When this is evaluated numerically, the pressure is calculated at each intermediate density using either the virial or compressibility expressions.

Combining the various expressions for the free energy and pressure, we can calculate the excess chemical potential along different paths: density-compressibility, Eqs. (22) with (19),

$$\beta\mu^e = \int_0^\rho \frac{1}{\rho'}\Big(\frac{\beta p}{\rho'} - 1\Big)d\rho' - \frac{1}{\rho}\int_0^\rho \rho' d\rho' \int c(\boldsymbol{r},\rho')d\boldsymbol{r}, \tag{23}$$

density-virial, Eqs. (22) with (18),

$$\beta\mu^e = \int_0^\rho \frac{1}{\rho'}\Big(\frac{\beta p}{\rho'} - 1\Big)d\rho' - \frac{\rho}{6}\int d\boldsymbol{r} r\frac{\partial\beta u(r)}{\partial r}g(r) \tag{24}$$

Kirkwood-compressibility, Eqs. (C1) with (19),

$$\begin{aligned} \beta\mu^e = \frac{\rho}{2}\int_0^1 d\lambda \int d\boldsymbol{r}\frac{\partial\beta u(r,\lambda)}{\partial\lambda}g(r,\lambda) \\ -\frac{1}{\rho}\int_0^\rho \rho' d\rho' \int c(\boldsymbol{r},\rho')d\boldsymbol{r}' \end{aligned} \tag{25}$$

or Kirkwood-virial, Eqs. (C1) with (18),

$$\begin{aligned} \beta\mu^e = \frac{\rho}{2}\int_0^1 d\lambda \int d\boldsymbol{r}\frac{\partial\beta u(r,\lambda)}{\partial\lambda}g(r,\lambda) \\ -\frac{\rho}{6}\int d\boldsymbol{r} r\frac{\partial\beta u(r)}{\partial r}g(r). \end{aligned} \tag{26}$$

*Gibbs-Duhem*

As with the Helmholtz free energy, a density dependent path of the chemical potential can be derived. This results in expressions using the virial,

$$\begin{aligned} \beta\mu^e = -\int_0^\rho d\rho' \Big[\frac{1}{3}\int d\boldsymbol{r} r\frac{\partial\beta u(r)}{\partial r}g(r) \\ + \frac{\rho'}{6}\int d\boldsymbol{r} r\frac{\partial\beta u(r)}{\partial r}\frac{\partial g(r)}{\partial\rho'}\Big], \end{aligned} \tag{27}$$

and compressibility paths,

$$\beta\mu^e = -kT\int_0^\rho d\rho' \int c(r,\rho')dr, \tag{28}$$

which are equivalent to the Gibbs-Duhem consistency equation, Eq. (8), (see Appendix A). However, if $\left(\frac{dp^v}{d\rho}\right)_T = \left(\frac{dp^c}{d\rho}\right)_T$ is not satisfied, then Eqs. (27) and (28) are not equivalent and may not agree with other expressions for the chemical potential. For example, HNC exhibits Gibbs-Duhem consistency when the viral pressure is used, Eq. (27), but not if the compressibility is used, Eq. (28).

## III. NUMERICAL PROCEDURE

In this work we consider a single-component fluid whose an interparticle potential is give by the Lennard-Jones potential

$$u(r) = 4\epsilon\left(\left(\frac{\sigma}{r}\right)^{12} - \left(\frac{\sigma}{r}\right)^{6}\right), \tag{29}$$

where $\sigma$ and $\epsilon$ are the size and energy parameters of the LJ potential, respectively. For all calculations we use reduced units, in which $\sigma$ and $\epsilon$ are the base units

for length and energy. This gives the reduced number density, $\rho^* = \rho\sigma^3$, temperature $T^* = k_B T/\epsilon$, and pressure, $p^* = p\sigma^3/\epsilon$.

Even when the free energy should be a path-independent property, the details of how the coupling constant is included in the potential energy are numerically important, as a simple linear coupling, $u(r,\lambda) = \lambda u(r)$, leads to large numerical errors. For this reason, a shifted and scaled LJ potential may be used [48]

$$u(r,\lambda) = 4\lambda\epsilon\left[\left(\frac{\sigma^2}{r^2+(1-\lambda)s}\right)^6 - \left(\frac{\sigma^2}{r^2+(1-\lambda)s}\right)^3\right] \tag{30}$$

where $s > 0$ is an arbitrary constant. In this approach, for each different value of $\lambda$ from 0 to 1, a new $g(r,\lambda)$ is computed. Numerically computing the Kirkwood excess free energy charging formula, Eq. (C1), then requires solving the OZ equation at different $\lambda$. Depending on the precision required, this can be computation onerous.

An in-house MATLAB [49] code was developed to solve the OZ equation, Eq. (1), using HNC, VM, and Eq. (11) bridge approximations to obtain thermodynamic properties of the LJ fluid using the theoretical formulations described in the preceding sections. A simple Picard iterative method was applied and the numerical tolerance for the root mean squared residual of the direct correlation functions during successive iterations was set at $10^{-10}$. All calculations were performed with the same number of grid points, $N = 8192$, and length parameter, $L = 32\sigma$. Thermodynamic quantities were computed for $T^* = 1.5, 2.74$, and 5 and $\rho\sigma^3 = 0.1$ to 1.1 in increments of 0.1.

At each temperature and pressure reported, pressure consistency was enforced by optimizing coefficients $(a, b_1)$ in Eq. (10) and $(\phi, \alpha)$ in Eq. (4) to satisfy the consistency condition. The pressure consistency equation was converged to $|p^v - p^c| \leq 10^{-6}$ using the 'fminsearch' multidimensional unconstrained nonlinear minimization routine of MATLAB. This required calculating the pressure from the virial and compressibility routes for each set of coefficients proposed by the minimizer. For the virial pressure, Eq. (18) was use directly. To calculated the compressibility pressure, Eq. (20) was employed where the trial coefficients were fixed for all intermediate densities, $\rho'$, in the integral. HNC was excluded from pressure consistency enforcement since it has no adjustable parameters.

Numerical calculations of the pressure, free energy, and chemical potential used the mid-point integration with step sizes $d\lambda = 0.005$ and $d\rho' = 0.025$ for the Kirkwood charging and thermodynamic integration formulas, respectively. Bridge function coefficients were held constant for each of these calculations. For Eq. (30), $s = 0.5$ was used.

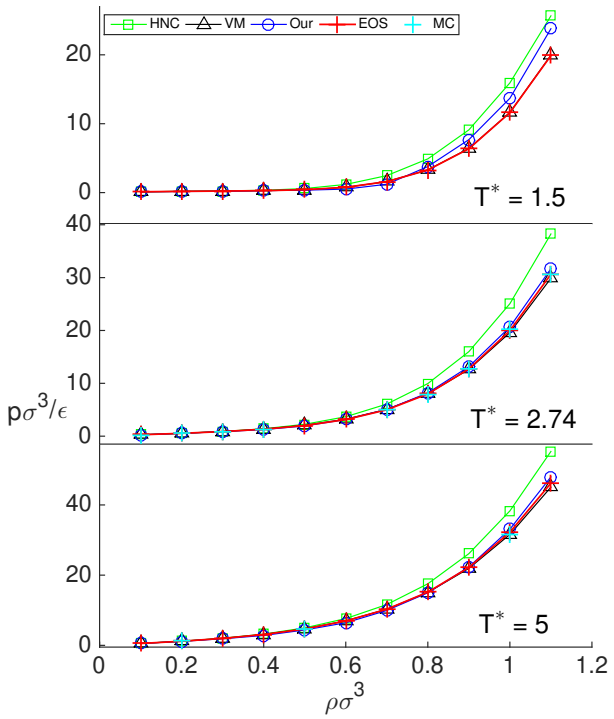


FIG. 1. Absolute pressure, $p\sigma^3/\epsilon$, as a function of density, $\rho\sigma^3$. Green, black and blue lines are from the HNC, VM and Eq. (11) bridge corrections respectively. Red crosses are from the equations of state in [31]. Cyan crosses are available MC data from [29] and [30] for $T^* = 2.74$ and 5.

## IV. RESULTS

### Pressure consistency

In Table I we compare pressures obtained from HNC, VM, and Eq. (11) bridge approximations for the LJ potential at $\rho\sigma^3 = 0.9$ and $T^* = 1.5, 2.74$ and 5. As expected, both VM and Eq. (11) show virial-compressibility consistency while HNC does not. Furthermore, while both VM and (11) are within a few percent of MC and EOS data [29–31] and each other at $T^* = 2.74$ and 5, HNC values differ considerably at all temperatures. At $T^* = 1.5$, Eq. (11) is still an improvement over HNC but has increased relative error.

We note that if we use $dp^v = dp^c$ consistency instead, the obtained numerical values for both pressures would be close, but inconsistent. For example, for the LJ potential at $T^* = 2.74$ and $\rho^* = 0.9$, the VM approximation gives $p^v\sigma^3/\epsilon = 12.70$ and $p^c\sigma^3/\epsilon = 13.05$ while our closure gives $p^v\sigma^3/\epsilon = 12.94$ and $p^c\sigma^3/\epsilon = 13.92$. Therefore, we did not employ $dp^v = dp^c$ consistency in this work.

As seen in Figure 1, the pressure for all three models is in good agreement with EOS data at low densities,

TABLE I. The pressure, $p\sigma^3/\epsilon$, from virial and compressibility routes for the LJ potential at $\rho\sigma^3 = 0.9$.

| | $T^* = 1.5$ | | | $T^* = 2.74$ | | | $T^* = 5$ | | |
|---|---|---|---|---|---|---|---|---|---|
| | HNC | Eq. (11) | VM | HNC | Eq. (11) | VM | HNC | Eq. (11) | VM |
| Virial | 9.104 | 7.688 | 6.421 | 15.99 | 13.15 | 12.64 | 26.12 | 22.32 | 21.92 |
| Compressibility | 3.781 | 7.688 | 6.421 | 9.415 | 13.15 | 12.64 | 18.12 | 22.32 | 21.92 |
| MC | | | | | 12.68[29] | | | | |
| EOS | | 6.365[31] | | | 12.72[31] | | | 22.19[31] | |

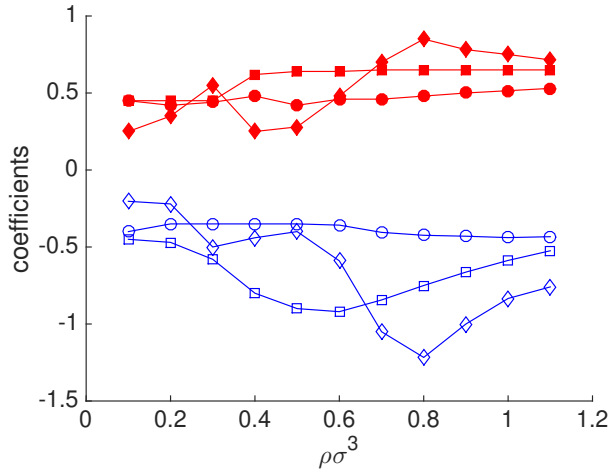


FIG. 2. Coefficients $a$ (red, filled) and $b_1$ (blue, unfilled) for Eq. (11) vs $\rho\sigma^3$ at $T^* = 1.5$ (diamonds), 2.74 (squares) and 5 (circles).

regardless of temperature. HNC, however, diverges from the EOS as the density increases, always overestimating the pressure, while VM stays within a few percent. Eq. (11) also behaves like VM for $T^* = 2.74$ and 5, tracking the EOS pressure within a few percent. However, at $T^* = 1.5$, Eq. (11) predicts excessively high pressures at high densities.

Figure 2 shows optimized values of coefficients $(a, b_1)$ of Eq. (10) vs $\rho\sigma^3$, which are obtained by enforcing viral and compressibility pressure consistency, Eq. (5). As seen here, the coefficients have both a temperature and pressure dependence though it appears to be diminished as density increases.

As with other closure approximations that enforce pressure consistency in this manner, including VM, there is no guarantee of uniqueness in the parameters found by minimization since the function is nonlinear. This is particularly true at low densities, where more than one pair of values $(a, b_1)$ may be found to satisfy the consistency criterion. However, at low densities, the effect of the bridge correction is small. For high densities, the range of $(a, b_1)$ pairs is much smaller. The result is that small variations can be found that depend on the initial guess but they are insignificant in practice.

TABLE II. Internal energy-pressure consistency for the LJ potential at $\rho\sigma^3 = 0.9$.

| | $T^* = 2.74$ | | | $T^* = 5$ | | |
|---|---|---|---|---|---|---|
| | HNC | Eq. (11) | VM | HNC | Eq. (11) | VM |
| $\rho^2 \left(\frac{\partial \beta E/N}{\partial \rho}\right)_T$ | 0.910 | 0.550 | 0.120 | 1.267 | 0.949 | 0.563 |
| $-T \left(\frac{\partial \beta p}{\partial T}\right)_\rho$ | 0.910 | 0.550 | 0.099 | 1.267 | 0.949 | 0.675 |

### Energy-pressure consistency

Table II shows the consistency of pressure and internal energy through density and temperature derivatives, as given in Eq. (6). As the virial pressure is used, both HNC and Eq. (11) show consistency while VM does not. If the pressure was calculated from the compressibility route, the results for Eq. (11) would be unaffected but HNC would fail to show consistency.

### Chemical potential and Helmholtz free energy

To test the path independence of our new closure, we calculated the excess Helmholtz free energy $A^e/\epsilon$ using the Kirkwood charging formula Eq. (C1), density integration Eq. (22) and the respective analytical formulas, Eqs. (12), (13), and (14). In Table III we show the values for $A^e/\epsilon$ at $T^* = 1.5, 2.74$ and 5 for $\rho\sigma^3 = 0.9$. As expected, results from HNC and Eq. (11) show no path dependence. The VM results, however, are path-dependent, with the Kirkwood and density integration formulas giving different, but close, values. The semi-analytical expression for VM is not consistent with the Kirkwood values, as it has a different coupling parameter, though it gives reasonable values. In contrast to the calculated pressure, Eq. (11) has the best agreement with EOS at the values at low temperatures while VM performs better at high temperatures. HNC over estimates the Helmholtz free energy in all cases and has the largest relative error.

Results for the excess Helmholtz free energy over a range of densities are shown in Figure 3 for temperatures $T^* = 1.5, 2.74$ and 5. HNC overestimates the free energy while the new bridge approximation tends to underestimate the free energy at higher densities. This is most apparent at $T^* = 2.74$ but the same behavior is also observed at $T^* = 5$. Only values for the

TABLE III. The excess Helmholtz free energy, $A^e/\epsilon$, per particle for the LJ potential at $\rho\sigma^3 = 0.9$.

| | $T^* = 1.5$ | | | $T^* = 2.74$ | | | $T^* = 5$ | | |
|---|---|---|---|---|---|---|---|---|---|
| | HNC | Eq. (11) | VM | HNC | Eq. (11) | VM | HNC | Eq. (11) | VM |
| Kirkwood (Eq. (C1)) | 0.115 | -0.752 | -0.600 | 3.904 | 2.251 | 2.630 | 9.570 | 7.315 | 8.009 |
| TI density (Eq. (22)) | 0.115 | -0.752 | -0.951 | 3.904 | 2.251 | 2.700 | 9.570 | 7.315 | 8.127 |
| Analytic (Eqs. (13), (12), (14)) | 0.115 | -0.752 | -0.493 | 3.904 | 2.251 | 2.961 | 9.570 | 7.315 | 8.194 |
| MC | | | | | 2.850[29] | | | | |
| EOS | | -0.720[31] | | | 2.850[31] | | | 8.248[31] | |

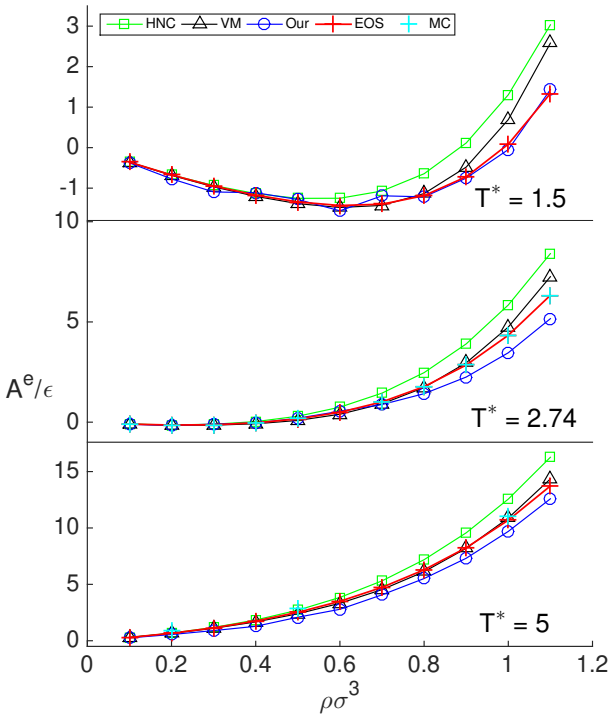


FIG. 3. Helmholtz free energy per particle, $A^e/\epsilon$, as a function of density, $\rho\sigma^3$. Green, black and blue lines are from the HNC, VM and Eq. (11) bridge corrections respectively. Red crosses are from the equations of state in [31]. Cyan crosses are MC simulation data taken from [29] and [30] for $T^* = 2.74$ and 5.

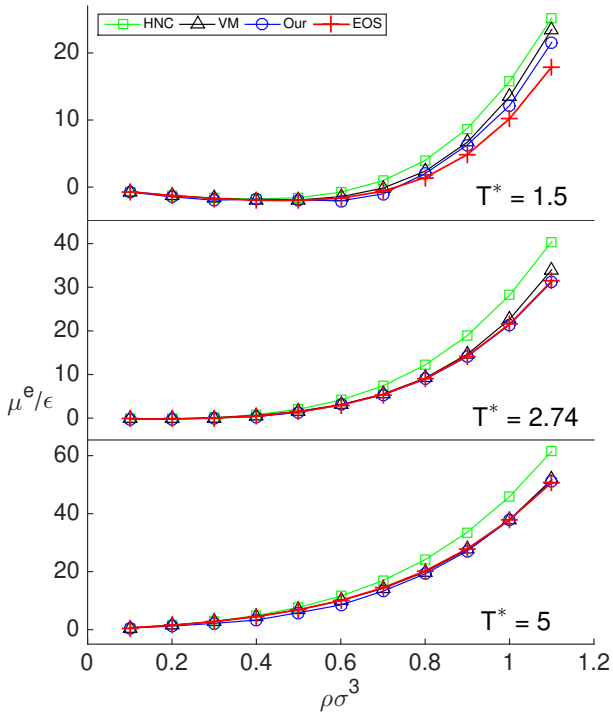


FIG. 4. Excess chemical potential, $\mu^e/\epsilon$, as a function of density, $\rho\sigma^3$. Green, black and blue lines are from the HNC, VM and Eq. (11) bridge corrections respectively. Red crosses are from the equations of state in [31].

analytical expression for the VM free energy are shown, but these are in good agreement with simulation at all temperatures and densities.

Several paths for the excess chemical potential are compared in Table IV for all three closure approximations. We can see that for all closures the agreement of the various numerical approaches with the analytic expression depends on which path was used. All closures display inconsistency between the virial and compressibility expressions for Gibbs-Duhem, Eqs. (27) and Eq. (28). This is due to inconsistency in the density derivative of the pressure, which all of these closures exhibit. We note that the virial expression for Gibbs-Duhem is consistent with the analytic expression for both HNC and Eq. (11).

Consistency for different thermodynamic routes for the free energy-pressure equation, Eq. (7), naturally depends on the consistency of the free energy and pressure of the respective closures. HNC has free energy consistency but not pressure consistency – as long as the virial path is used Gibbs-Duhem, free energy and pressure, and the analytic expressions all agree. Conversely, VM has pressure consistency but not free energy consistency, so Kirkwood and density paths to the free energy and chemical potential do not agree. However, density integration is consistent with the virial Gibbs-Duhem expression. Because Eq. (11) exhibits both free energy and pressure consistency, all routes agree, except for the compressibility Gibbs-Duhem expression.

TABLE IV. The excess chemical potential $\mu^e/\epsilon$ for the LJ potential at $\rho\sigma^3 = 0.9$.

| | $T^* = 1.5$ | | | $T^* = 2.74$ | | | $T^* = 5$ | | |
|---|---|---|---|---|---|---|---|---|---|
| | HNC | Eq. (11) | VM | HNC | Eq. (11) | VM | HNC | Eq. (11) | VM |
| Gibbs-Duhem | | | | | | | | | |
| Compressibility (Eq. (28)) | 1.479 | 6.693 | 5.505 | 9.811 | 13.77 | 14.52 | 22.32 | 27.33 | 27.80 |
| Virial (Eq. (27)) | 8.726 | 6.292 | 4.680 | 18.93 | 14.13 | 14.00 | 33.59 | 27.12 | 27.49 |
| Kirkwood-compressibility (Eq. (25)) | 2.816 | 6.291 | 5.035 | 11.62 | 14.13 | 13.93 | 24.70 | 27.12 | 27.38 |
| Kirkwood-virial (Eq. (26)) | 8.730 | 6.292 | 5.035 | 18.93 | 14.13 | 13.93 | 33.59 | 27.12 | 27.37 |
| Free energy and pressure | | | | | | | | | |
| TI density-compressibility (Eq. (23)) | 2.816 | 6.291 | 4.684 | 11.62 | 14.13 | 14.00 | 24.70 | 27.12 | 27.50 |
| TI density virial (Eq. (24)) | 8.730 | 6.292 | 4.684 | 18.93 | 14.13 | 14.00 | 33.59 | 27.12 | 27.49 |
| Analytic (Eqs. (16), (17), (15)) | | | | | | | | | |
| | 8.730 | 6.293 | 5.517 | 18.93 | 14.13 | 14.65 | 33.59 | 27.12 | 27.60 |
| EOS [31] | | 4.852 | | | 14.24 | | | 27.90 | |

VM and Eq. (11) have similar accuracy for the chemical potential over a range of temperatures and compare well to the EOS, as shown in Figure 4. Again, HNC over-estimates the MC data and is significantly higher than VM and Eq. (11). Analytic expressions were used for all three closures. Overall, Eq. (11) has better agreement with the excess chemical potential than it does with the Helmholtz free energy (Figure 3) especially at high temperatures and is similar to that observed for the pressure (Figure 1).

## V. DISCUSSION

Thermodynamically consistent behavior is an essential property for a successful theory of liquids. The primary result of this work is the development of a closure for the OZ equation that has both pressure and free energy consistency. While pressure consistent and free energy path independent closures have been developed before, this is the first time that a single closure has demonstrated both.

### A. Thermodynamic Consistency

To examine how satisfying both types of thermodynamic consistency can improve the predictive power of the OZ equation, we compared our results against VM and HNC closures. These alternately satisfy virial-compressibility pressure consistency (VM) or path independence for the free energy respectively (HNC) but not both. All other closures that we are aware of either satisfy only virial-compressibility pressure or free energy consistency. As expected, enforcing pressure consistency improves predictions of the pressure from VM and Eq. (11) compared to HNC, particularly at high temperature and density.

We have more routes to the free energy and chemical potential, which allows us to examine in greater detail the implications of thermodynamic consistency or lack thereof. Because Eq. (11) satisfies the Kast criteria [20] and pressure consistency is enforced, all routes to the free energy and chemical potential provide consistent results, except for the Gibbs-Duhem expression using the compressibility, Eq. (28), which we discuss below. HNC does have internal energy-virial consistency but not pressure consistency, so any expression that uses the compressibility route is inconsistent but viral and Kirkwood results are consistent, which includes the analytic expressions. The VM closure only exhibits pressure consistency, so analytic expressions are simply approximations. Numeric results may agree with each other but only when the only difference is whether the pressure is calculated from the viral or compressibility route.

To achieve consistency for all routes to the chemical potential tested here it is necessary to have consistency of the density derivative of the pressure, $\left(\frac{dp^v}{d\rho}\right)_T = \left(\frac{dp^c}{d\rho}\right)_T$, while satisfying pressure consistency. None of the three closures satisfy this, as is demonstrated by the results for the Gibbs-Duhem expression for the chemical potential, Table IV. For this additional consistency, it is necessary that the free parameters in the bridge be independent of density. We see this at $T^* = 5$, where the coefficients for Eq. (11) change very little with density (Figure 2) and Gibbs-Duhem consistency is nearly achieved (Table IV).

An additional consequence of free energy path independence is that we were able to derive analytical, closed form formulas for the excess free energy and excess chemical potential for our new closure. This allows the excess free energy and excess chemical potential to be computed without the Kirkwood charging or any other numerical form of thermodynamic integration. Indeed, we find that these formulas are completely consistent with the various numerical paths we have tested for Eq. (12). This is in contrast to the approximate formulas for VM, which are in poor agreement with various numerical results.

### B. Partial molar volume correction

Some physical insight to can be gained by comparing our new closure to the various partial molar volume based corrections that have been proposed for 3D-RISM theory and molecular density functional theory (MDFT) [24–27]. These are modifications to the usual closure specific expressions for the chemical potential and are not bridge corrections. These all have a similar form to UC applied to HNC,

$$\beta\mu^{\mathrm{UC}} = \beta\left\{\mu^{\mathrm{HNC}} + a'\rho v + b'\right\},$$

where $a'$ and $b'$ are parameters fit to experiment and $v$ is the PMV of the solute, may be interpreted as by compensating for mechanical work (pressure-volume) required to introduce a solute. From this interpretation, we have $a' = P_{\mathrm{contact}}/\rho$. Due to pressure inconsistencies in HNC, $P_{\mathrm{contact}}$ is not equal to the virial or compressibility pressure but is the contact pressure between the solute and solvent [27, 50, 51]. Like the virial and compressibility pressures, the contact pressure for HNC is too high and corrections like UC are employed to compensate for this.

Comparing our expression for the chemical potential, Eq. (15), to UC, we find that the coefficients are related as $a \approx -\beta a'$ and $b_1 \approx \beta a'$ and, by analogy, $a \approx -b_1 \approx -\beta P_{\mathrm{contact}}/\rho$ (see Appendix D). In agreement with this, Figure 2 shows that $a \approx -b_1$. This observation suggests it may be possible to replace the $b_1$ coefficient with $-a$.

PMV corrections have been used successfully for water ( e.g., [25–27, 52–54]) and other solvents (e.g., [55–58]). Because room temperature and atmospheric pressure are typical physical conditions for solvated biological and non-biological systems, we anticipate that this closure will work well where PMV corrections have been used before. For example, simulations of water are commonly performed at $T = [298.15\,\mathrm{K}$ and $\rho = 997\,\mathrm{kg/m^3}$ or $T^* = 3.82$ and $\rho^* = 1.06$ using the SPC/E model [59]. These conditions correspond to the highest temperatures and densities we tested, where we observed pressures and chemical potentials in good agreement with the equation of state. Non-polar solvents, such as cyclohexane, have similar reduced temperatures but lower densities than water for similar calculations. Indeed, we expect that this closure will perform well for typical solvation free energy calculations for which PMV corrections have been used in the past.

## VI. CONCLUSION

In this work we have proposed a new closure equation, Eq. (10), for the Ornstein-Zernike equation that satisfies both virial-compressibility pressure consistency and path independence for the chemical potential and free energy. As a consequence, this closure also exhibits internal energy-pressure, free energy-pressure, and Gibbs-Duhem consistency. Consistency was demonstrated by calculating solutions to the Ornstein-Zernike equation with our new closure truncated at the first term of the summation, Eq. (11), for the Lennard-Jones potential at thermodynamic parameters $T^* = 1.5, 2.74$ and 5, and $\rho\sigma^3 = 0.1$ to 1.1. In addition, we were able to derive closed form expressions for the free energy and chemical potential. We anticipate that this closure will be particularly useful for calculations of common solvents in 3D-RISM and molecular CDFT calculations where PMV corrections are currently used.


## ACKNOWLEDGEMENT

This material is based upon work supported by the National Science Foundation (NSF) under Grant No. (1566638) and a Cottrell Scholar Award from the Research Corporation for Science Advancement (RCSA).


## Appendix A: Density derivative path to the chemical potential

Following [60], when we hold the temperature constant, starting from the thermodynamic identity

$$dG = V\,dp - S\,dT,$$

we have

$$\left(\frac{\partial G}{\partial p}\right)_T = V$$
$$\left(\frac{\partial \mu}{\partial p}\right)_T = \rho^{-1}$$
$$\left(\frac{\partial \mu}{\partial \rho}\right)_T \left(\frac{\partial \rho}{\partial p}\right)_T = \rho^{-1}$$
$$\left(\frac{\partial \mu^e}{\partial \rho}\right)_T + \left(\frac{\partial \mu^i}{\partial \rho}\right)_T = \rho^{-1}\left[\left(\frac{\partial p^e}{\partial \rho}\right)_T + \left(\frac{\partial P^i}{\partial \rho}\right)_T\right].$$

In the second step we have the Gibbs-Duhem relation and in the last step we have split the chemical potential into excess, $e$, and ideal, $i$, contributions. For the ideal contribution on the right hand side we have

$$\left(\frac{\partial p^i}{\partial \rho}\right)_T = \frac{\partial}{\partial \rho}\rho kT = kT$$

where we have used the ideal gas law. For the excess chemical potential, we then have

$$\left(\frac{\partial \mu^e}{\partial \rho}\right)_T = \rho^{-1}\left[\left(\frac{\partial p}{\partial \rho}\right)_T - kT\right]$$
$$\mu^e = \int_0^\rho d\rho' \frac{1}{\rho'}\left[\left(\frac{\partial p}{\partial \rho'}\right)_T - kT\right]$$

We may use either Eq. (18) or Eq. (19) for the derivative of the pressure. Using Eq. (18), we have

$$\begin{aligned}\mu^e &= \int_0^\rho d\rho' \frac{1}{\rho'}\Big[kT\Big(1-2\frac{\rho'}{6}\int d\boldsymbol{r} r\frac{\partial\beta u(r)}{\partial r}g(r)\\ &\quad -\frac{\rho'^2}{6}\int d\boldsymbol{r} r\frac{\partial\beta u(r)}{\partial r}\frac{\partial g(r)}{\partial\rho'}\Big)-kT\Big]\\ &= -\int_0^\rho d\rho'\Big[\frac{1}{3}\int d\boldsymbol{r} r\frac{\partial\beta u(r)}{\partial r}g(r)\\ &\quad +\frac{\rho'}{6}\int d\boldsymbol{r} r\frac{\partial\beta u(r)}{\partial r}\frac{\partial g(r)}{\partial\rho'}\Big].\end{aligned}$$

Using Eq. (19) we have

$$\begin{aligned}\mu^e &= \int_0^\rho d\rho'\frac{1}{\rho'}\left[kT\left(1-\rho'\int c(r,\rho')d\boldsymbol{r}\right)-kT\right]\\ &= -kT\int_0^\rho d\rho'\int c(r,\rho')d\boldsymbol{r}\end{aligned}$$

which is the result obtained by [60].

### Appendix B: Free energy path independence and closed-form chemical potential

The most common approach to calculating the chemical potential, $\mu^e$, (i.e., the Gibbs free energy per particle) is through the Kirkwood charging formula [61, 62],

$$\begin{aligned}\beta\mu &= \beta\mu^{id}+\beta\mu^e\\ &= \beta\mu^{id}+\rho\int_0^1 d\lambda\int d\boldsymbol{r}\frac{\partial\beta u_{\mathrm{UV}}(r,\lambda)}{\partial\lambda}g_{\mathrm{UV}}(r,\lambda),\end{aligned}\quad\text{(B1)}$$

where $\beta\mu^{id}$ and $\beta\mu^e$ are the ideal and excess chemical potentials. In the language of charging technique, one may add one (marked) solute particle, U, from infinity to a given point into the $N-1$ particle solvent system solvent, V, and the intermolecular interactions between them scales until the added particle is not distinguished from the others. For the Kirkwood approach, $\lambda$ scales interactions of one (marked) particle with others, that is, when $\lambda=0$, the particle is removed and when $\lambda=1$, the particle is fully coupled to the system. The integral may be computed analytically if $\beta\mu^e$ is independent of how $\lambda$ scales the interaction; i.e., it is path independent.

To ensure path independence in Eq. (B1), Kast [20] uses a variational approach to obtain a constrained formula for the excess chemical potential

$$\begin{aligned}\mu^e = \int_0^1\int \rho(h+1)\frac{\partial u}{\partial\lambda}+pP+vV\,d\mathbf{r}\,d\lambda\\ +\frac{q}{(2\pi)^3}\int_0^1\int Q\,d\mathbf{k}\end{aligned}\quad\text{(B2)}$$

where, in the general case,

$$\begin{aligned}P &= \exp(-\beta u+\gamma+B)-h-1,\\ V &= h-c-\gamma,\\ Q &= \rho\hat{c}\frac{\partial\hat{c}}{\partial\lambda}\left(1+\frac{\rho\hat{c}}{1-\rho\hat{c}}\right)-\frac{\partial\hat{c}}{\partial\lambda}\rho\hat{h}\end{aligned}$$

and $p$, $v$, and $q$ are variational parameters to be solved for. For path-independence to be satisfied, the functional derivatives of Eq. (B2) with respect to $h$, $c$, $\gamma$, and $u$ must be zero:

$$\frac{\partial\mu^e}{\partial h}=\rho\frac{\partial u}{\partial\lambda}+p\left[\frac{\partial B}{\partial h}(h+1)-1\right]-q\rho\frac{\partial c}{\partial\lambda}+v=0,\quad\text{(B3)}$$

$$\frac{\partial\mu^e}{\partial c}=p\frac{\partial B}{\partial c}(h+1)+q\rho\frac{\partial h}{\partial\lambda}-v=0,\quad\text{(B4)}$$

$$\frac{\partial\mu^e}{\partial\gamma}=p\left(\frac{\partial B}{\partial\gamma}+1\right)(h+1)-v=0,\quad\text{(B5)}$$

$$\frac{\partial\mu^e}{\partial u}=p\left(\frac{\partial B}{\partial u}-\beta\right)(h+1)-\rho\frac{\partial h}{\partial\lambda}=0.\quad\text{(B6)}$$

This system of equations is then solved for $p$, $v$ and $q$, giving

$$p=\rho\frac{\partial h}{\partial\lambda}\frac{1}{\left(\frac{\partial B}{\partial u}-\beta\right)(h+1)},\quad\text{(B7)}$$

$$v=\rho\frac{\partial h}{\partial\lambda}\frac{\frac{\partial B}{\partial\gamma}+1}{\frac{\partial B}{\partial u}-\beta},\quad\text{(B8)}$$

$$q=\frac{\frac{\partial B}{\partial\gamma}-\frac{\partial B}{\partial c}+1}{\frac{\partial B}{\partial u}-\beta}.\quad\text{(B9)}$$

For a closure with bridge approximation given by Eq. (10) we may obtain

$$\begin{aligned}p &= -\beta^{-1}(h+1)^{-1}\frac{\partial h}{\partial\lambda}\qquad v=-\beta^{-1}\rho\frac{\partial h}{\partial\lambda},\\ q &= -\beta^{-1}(1-a).\end{aligned}\quad\text{(B10)}$$

From the equation for $q$ in Eq. (B10) it is seen that the proposed bridge approximation Eq. (10) has satisfied this path independence condition.

Combining Eqs. (B3) with (B1) and $p$, $v$ and $q$ we have

$$\begin{aligned}\mu^e = \mu^{\mathrm{HNC}}-\rho\int_0^1\int d\mathbf{r}\,d\lambda\frac{1}{\left(\frac{\partial B}{\partial u}-\beta\right)}\\ \left\{\frac{\partial h}{\partial\lambda}(h+1)\left[\frac{\partial B}{\partial h}+\frac{\partial B}{\partial\gamma}\right]\right.\\ \left.-\frac{\partial c}{\partial\lambda}(h+1)\left(\frac{\partial B}{\partial t}-\frac{\partial B}{\partial c}\right)\right\}.\end{aligned}\quad\text{(B11)}$$

It is straightforward to extend this to multicomponent 1D- or 3D-RISM cases.

For the specific case of Eq. (10) we have

$$\frac{\partial B}{\partial u} = 0, \qquad \frac{\partial B}{\partial \gamma} = 0,$$
$$\frac{\partial B}{\partial c} = a, \qquad \frac{\partial B}{\partial h} = \sum_{i=1} i b_i h^{i-1},$$

and Eq. (B11) reduces to

$$\mu^e = \mu^{\rm HNC} - \frac{\rho}{\beta}\int d\mathbf{r} \left\{ b_1 h + \sum_{i=2}\left(b_i + b_{i-1}\left(1-\frac{1}{i}\right)\right)h^i - \frac{1}{2}ahc + ac \right\} \tag{B12}$$

### Appendix C: Closed form expressions for free energy and chemical potential

As with the chemical potential, the Helmholtz free energy can also be computed with the Kirkwood charging technique [61, 62], in which the free energy difference between two different states is calculated by gradually "switched between" the two different Hamiltonians using the coupling parameter $\lambda$. When $\lambda = 0$, the system is represented by a Hamiltonian corresponding to the initial state, and for $\lambda = 1$ by a Hamiltonian corresponding to the final state. Then the excess Helmholtz free energy, $A^e$, is obtained in terms of thermodynamic integration with the Kirkwood charging formula,

$$\frac{\beta A^e}{N} = \frac{\rho}{2}\int_0^1 d\lambda \int d\boldsymbol{r} \frac{\partial \beta u(r,\lambda)}{\partial \lambda} g(r,\lambda). \tag{C1}$$

The manner in which $\lambda$ is coupled to $u(r,\lambda)$ determines the computational path. To eliminate a derivative of $\partial u/\partial\lambda$ in the Kirkwood charging formulas, Eqs. (C1) and (B1), we begin with the exact expression

$$(1+h(\boldsymbol{r},\lambda)) = e^{-\beta u(\boldsymbol{r},\lambda)+h(\boldsymbol{r},\lambda)-c(\boldsymbol{r},\lambda)+B(\boldsymbol{r},\lambda)}. \tag{C2}$$

Taking the derivative of both sides we arrive at

$$\beta(1+h)\frac{\partial u}{\partial\lambda} = \frac{\partial}{\partial\lambda}\Big(\frac{1}{2}h^2 - c + B\Big) - h\frac{\partial c}{\partial\lambda} + h\frac{\partial B}{\partial\lambda}. \tag{C3}$$

Inserting Eq. (C3) into the Kirkwood charging formula for the excess free energy, Eq. (C1), we have

$$\frac{\beta A^e}{N} = \frac{\rho}{2}\int d\boldsymbol{r}\Big(\frac{1}{2}h^2 - c + B\Big) - \frac{\rho}{2}\int_0^1 d\lambda\int d\boldsymbol{r} h\frac{\partial c}{\partial\lambda} + \frac{\rho}{2}\int_0^1 d\lambda\int d\boldsymbol{r} h\frac{\partial B}{\partial\lambda} \tag{C4}$$

In the second integral we need to express $h$ in terms of $c$ in order to integrate over $\lambda$, that is,

$$\begin{aligned}\int_0^1 d\lambda\int d\boldsymbol{r} h\frac{\partial c}{\partial\lambda} &= \int_0^1 d\nu\int d\boldsymbol{r} hc \\ &= \frac{1}{8\pi^3}\int_0^1 d\nu\int d\boldsymbol{k}\,\widehat{h(\nu c)}\,\hat{c} \\ &= \frac{1}{8\pi^3}\int_0^1 d\nu\int d\boldsymbol{k}\frac{\nu\hat{c}}{1-\rho\nu\hat{c}}\hat{c} \\ &= \frac{1}{8\pi^3}\int d\boldsymbol{k}\hat{c}^2\int_0^1 d\nu\frac{\nu}{1-\rho\nu\hat{c}} \\ &= -\frac{1}{8\pi^3}\frac{1}{\rho}\int d\boldsymbol{k}\Big[\hat{c} + \frac{1}{\rho}\ln|1-\rho\hat{c}|\Big].\end{aligned} \tag{C5}$$

Here we used $(\partial c/\partial\lambda)d\lambda = c d\nu$ and $\widehat{\nu c} = \nu\hat{c}$ and Parseval's Theorem $\int a(\boldsymbol{r})b(\boldsymbol{r})d\boldsymbol{r} = (1/8\pi^3)\int \hat{a}\hat{b}d\boldsymbol{k}$ [42].

For the third integral, we can write

$$\int\int_0^1 h\frac{\partial B}{\partial h}d\lambda d\boldsymbol{r} = \int hB d\boldsymbol{r} - \int\int_0^1 B\frac{\partial h}{\partial\lambda}d\lambda d\boldsymbol{r}. \tag{C6}$$

If we assume that $h(r,\lambda) \approx \lambda h(r)$ and use expression Eq. (10) for $B(r)$, the second integral of Eq. (C6) becomes

$$\begin{aligned}\int\int_0^1 ac\frac{\partial h}{\partial\lambda}d\lambda d\boldsymbol{r} + \sum_i b_i\int\int_0^1 h^i\frac{\partial h}{\partial\lambda}d\lambda d\boldsymbol{r} \\ = \frac{1}{8\pi^3}\frac{a}{\rho}\int d\boldsymbol{k}\Big[\hat{h} - \frac{1}{\rho}\ln|1+\rho\hat{h}|\Big] \\ + \int d\boldsymbol{r}\sum_i\frac{b_i}{i+1}h^{i+1}.\end{aligned} \tag{C7}$$

Combining Eqs. (C6)-(C7), we have

$$\begin{aligned}\frac{\beta A^e}{N} = \frac{\rho}{2}\int d\boldsymbol{r}\Big(\frac{1}{2}h^2 - c\Big) \\ + \frac{1}{2}\frac{1}{8\pi^3}\int d\boldsymbol{k}\Big[\hat{c} + \frac{1}{\rho}\ln|1-\rho\hat{c}|\Big] \\ + \frac{\rho}{2}\int d\boldsymbol{r} gB \\ - \frac{a}{2}\frac{1}{8\pi^3}\int d\boldsymbol{k}\Big[\hat{h} - \frac{1}{\rho}\ln|1+\rho\hat{h}|\Big] \\ - \frac{\rho}{2}\int\sum_i\frac{b_i}{i+1}h^{i+1}d\mathbf{r}.\end{aligned} \tag{C8}$$

For the VM closure, we may follow the same procedure with the observation that that a particular coupling is selected. Proceeding with this understanding, the second

integral of Eq.(C6) becomes

$$\begin{aligned}\int_0^1 d\lambda \int B\frac{\partial h}{\partial \lambda}d\boldsymbol{r} &= \int_0^1 d\nu \int Bhd\boldsymbol{r} \\ &= \frac{1}{8\pi^3}\int_0^1 d\nu \int d\boldsymbol{k}\,\widehat{B(\nu h)}\,\hat{h} \\ &= -\frac{1}{2}\frac{1}{8\pi^3}\int d\boldsymbol{k}\hat{h}\int_0^1 d\nu \\ &\quad \times \frac{\phi\left(\rho\nu^2\hat{h}^2/(1+\rho\nu\hat{h})\right)^2}{1+\alpha\nu^2\hat{h}^2/(1+\rho\nu\hat{h})}. \end{aligned} \tag{C9}$$

Then combining Eqs. (C6) and (C9) we have

$$\begin{aligned}\frac{\beta A^e}{N} &= \frac{\rho}{2}\int d\boldsymbol{r}\Big(\frac{1}{2}h^2 - c\Big) \\ &\quad + \frac{1}{2}\frac{1}{8\pi^3}\int d\boldsymbol{k}\Big[\hat{c} + \frac{1}{\rho}\ln|1-\rho\hat{c}|\Big] \\ &\quad + \frac{\rho}{2}\int d\boldsymbol{r}gB \\ &\quad + \frac{\rho}{4}\frac{1}{8\pi^3}\int d\boldsymbol{k}\hat{h}\int_0^1 d\nu \frac{\phi(\rho\nu^2\hat{h}^2/(1+\rho\nu\hat{h}))^2}{(1+\alpha\nu^2\hat{h}^2/(1+\rho\nu\hat{h}))}. \end{aligned} \tag{C10}$$

For the excess chemical potential $\beta\mu^e$, from Eqs. (B1) and (C3), we can write

$$\begin{aligned}\beta\mu^e &= \rho\int d\boldsymbol{r}\Big(\frac{1}{2}h_{\rm UV}^2 - c_{\rm UV} + B_{\rm UV}\Big) \\ &\quad - \rho\int_0^1 d\lambda\int d\boldsymbol{r}h_{\rm UV}\frac{\partial c_{\rm UV}}{\partial\lambda} \\ &\quad + \rho\int_0^1 d\lambda\int d\boldsymbol{r}h_{\rm UV}\frac{\partial B_{\rm UV}}{\partial\lambda}. \end{aligned} \tag{C11}$$

Where UV denotes correlation functions between a marked solute particle, U, and the bulk solvent liquid, V. While this looks almost identical to Eq. (C4), in this case $\lambda$ scales the interaction between the single marked particle and the liquid rather than all of the interactions in the liquid. The OZ equation for the solute particle is then [63]

$$h_{\rm UV}(r) = c_{\rm UV}(r) + \rho\int c_{\rm UV}(|\boldsymbol{r}-\boldsymbol{r}'|)h_{\rm VV}(\boldsymbol{r}')d\boldsymbol{r}'.$$

Because $h_{\rm VV}(\boldsymbol{r})$ does not depend on $\lambda$, we may choose that $c(r,\lambda) = \lambda c(r)$, which leads to

$$\begin{aligned}\beta\mu^e &= \rho\int d\boldsymbol{r}\Big(\frac{1}{2}h^2 - c - \frac{1}{2}hc\Big) + \rho\int d\boldsymbol{r}gB \\ &\quad - \rho\int d\boldsymbol{r}\Big[\frac{1}{2}ahc + (\sum_i \frac{b_i}{i+1}h^{i+1})\Big] \end{aligned} \tag{C12}$$

In evaluation of the excess chemical potential $\beta\mu^e$ for the VM approximation, the second integral of Eq. (C6) becomes

$$\int B\frac{\partial h}{\partial\lambda}d\lambda d\boldsymbol{r} = \int B'hd\boldsymbol{r} \approx \int \frac{B}{3}hd\boldsymbol{r}. \tag{C13}$$

Here $B'$ denotes the series of integrated bridge diagrams with the $h$ bond removed [42]. Combining Eqs. (C6) and (C13), and inserting them in Eq. (C11), we have

$$\beta\mu^e = \rho\int d\boldsymbol{r}\Big(\frac{1}{2}h^2 - c - \frac{1}{2}hc\Big) + \rho\int d\boldsymbol{r}(B + \frac{2h}{3}B). \tag{C14}$$

## Appendix D: Connection to PMV corrections

The analytic expression for the excess chemical potential, Eq. (15), bears a strong resemblance to PMV corrections that have been used with 3D-RISM theory and molecular density functional theory [24–27]. To see the connection, we first expand Eq. (15) to the form

$$\begin{aligned}\beta\mu^e &= \beta\mu^{\rm HNC} + a\rho\int d\mathbf{r}c(r) + \frac{1}{2}a\rho\int d\mathbf{r}c(r)h(r) \\ &\quad + \sum_i b_i\rho\int d\mathbf{r}\left[h^i(r) + \left(\frac{i}{i+1}\right)h^{i+1}(r)\right] \end{aligned} \tag{D1}$$

In the case that we truncate the summation at $b_1$, this becomes

$$\begin{aligned}\beta\mu^e &= \beta\mu^{\rm HNC} + a\rho\int d\mathbf{r}c(r) + b_1\rho\int d\mathbf{r}h(r) \\ &\quad + \frac{1}{2}a\rho\int d\mathbf{r}c(r)h(r) + b_1\frac{\rho}{2}\int d\mathbf{r}h^2(r). \end{aligned} \tag{D2}$$

The most general of the PMV corrections is the Universal Correction [24], which can be applied to the HNC expression as

$$\beta\mu^{\rm UC} = \beta\left\{\mu^{\rm HNC} + a'\rho v + b'\right\}, \tag{D3}$$

where $a'$ and $b'$ are parameters fit to experiment and $v$ is the PMV,

$$v = k_{\rm B}T\chi_T\left(1 - \rho\int c\left(\mathbf{r}\right)d\mathbf{r}\right). \tag{D4}$$

It is useful to expand $v$ using an alternate expression for the isothermal compressibility [32, 33, 64],

$$\chi_T = \frac{\beta}{\rho} + \beta\int h\,d\mathbf{r}. \tag{D5}$$

Combining (D3), (D4), and (D5), we have

$$\begin{aligned}\beta\mu^{\rm UC} &= \beta\left\{\mu^{\rm HNC} - a'\rho\int d\mathbf{r}c(r) + a'\rho\int d\mathbf{r}h(r)\right. \\ &\quad \left. -a'\rho^2\left(\int d\mathbf{r}h(r)\right)\left(\int d\mathbf{r}c(r)\right) + a' + b'\right\} \end{aligned} \tag{D6}$$

The similarity is most easily seen between Eqs. (D2) and (D6), were we can say that $a \approx -\beta a'$ , $b_1 \approx \beta a'$, and $a' + b' \approx b_1\frac{\rho}{2}\int d\mathbf{r}h^2(r)$. For the general case of Eq. (D1), we have instead

$$\begin{aligned}a' + b' &\approx b_1\frac{\rho}{2}\int d\mathbf{r}h^2(r) \\ &\quad + \sum_{i=2} b_i\rho\int d\mathbf{r}\left[h^i(r) + \left(\frac{i}{i+1}\right)h^{i+1}(r)\right]. \end{aligned}$$

[1] L. S. Ornstein and F. Zernike, Proc. Natl. Acad. Sci. USA **7**, 793 (1914)
[2] R. Evans, Adv. in Phys. **28**, 143 (1979)
[3] D. Chandler and H. C. Andersen, J. Chem. Phys. **57**, 1930 (1972)
[4] F. Hirata and P. J. Rossky, Chem. Phys. Lett. **83**, 329 (1981)
[5] J. Perkyns and B. M. Pettitt, J. Chem. Phys. **97**, 7656 (1992)
[6] D. Beglov and B. Roux, J. Phys. Chem. B **101**, 7821 (1997)
[7] A. Kovalenko and F. Hirata, J. Chem. Phys. **110**, 10095 (1999)
[8] L. Blum and A. J. Torruella, J. Chem. Phys. **56**, 303 (1972)
[9] L. Blum, J. Chem. Phys. **57**, 1862 (1972)
[10] S. Zhao, R. Ramirez, R. Vuilleumier, and D. Borgis, J. Chem. Phys. **134**, 194102 (2011)
[11] L. Verlet, Mol. Phys. **41**, 183 (1980)
[12] L. Verlet and D. Levesque, Mol. Phys. **46**, 969 (1982)
[13] G. A. Martynov and G. N. Sarkisov, Mol. Phys. **49**, 1495 (1983)
[14] F. J. Rogers and D. A. Young, Phys. Rev. A **30**, 999 (1984)
[15] G. Zerah and J. Hansen, J. Chem. Phys. **84**, 2336 (1986)
[16] P. Ballone, G. Pastore, G. Galli, and D. Gazzillo, Mol. Phys. **59**, 275 (1986)
[17] G. A. Martynov and A. G. Vompe, Phys. Rev. E **47**, 1012 (1993)
[18] D. Duh and A. D. J. Haymet, J. Chem. Phys. **103**, 2625 (1995)
[19] L. L. Lee, J. Chem. Phys. **103**, 9388 (1995)
[20] S. M. Kast, Phys. Rev. E **67**, 041203 (2003)
[21] T. Morita, Prog. Theor. Phys. **20**, 920 (1958)
[22] S. M. Kast and T. Kloss, J. Chem. Phys. **129**, 236101 (2008)
[23] I. S. Joung, T. Luchko, and D. A. Case, J. Chem. Phys. **138**, 044103 (2013)
[24] D. S. Palmer, A. I. Frolov, E. L. Ratkova, and M. V. Fedorov, J. Phys.: Cond. Matt. **22**, 492101 (2010)
[25] V. Sergiievskyi, G. Jeanmairet, M. Levesque, and D. Borgis, J. Chem. Phys. **143**, 184116 (2015)
[26] V. Sergiievskyi, G. Jeanmairet, M. Levesque, and D. Borgis, J. Chem. Phys. Lett. **5**, 1935 (2014)
[27] J. Johnson, D. A. Case, Y. Yamazaki, S. Gusarov, A. Kovalenko, and T. Luchko, J. Phys.: Cond. Matt. **28**, 344002 (2016)
[28] N. Choudhury and S. K. Ghosh, J. Chem. Phys. **116**, 8517 (2002)
[29] H. C. Andersen, D. Chandler, and J. D. Weeks, J. Chem. Phys. **56**, 3812 (1972)
[30] J. P. Hansen, Phys. Rev. A **2**, 221 (1970)
[31] M. Thol, G. Rutkai, A. Köster, R.Lustig, R. Span, and J. Vrabec, J. Phys. Chem. Ref. Data **45**, 023101 (2016)
[32] D. A. McQuarrie, *Statistical Mechanics*, University Press Books, (2010)
[33] J.-P. Hansen and I. R. McDonald, *Theory of Simple Liquids*, Academic Press, (2006)
[34] T. Morita and K. Hiroike, Prog. Theor. Phys. **23**, 1003 (1960)
[35] J. D. Weeks, D. Chandler, and H. C. Andersen, J. Chem. Phys. **54**, 5237 (1971)
[36] P. Attard and G. N. Patey, J. Chem. Phys. **92**, 4970 (1990)
[37] J. Perkyns and B. M. Pettitt, Theor. Chem. Acc. **96**, 61 (1997)
[38] E. Lomba and L. L. Lee, Int. J. Thermo. **17**, 663 (1996)
[39] L. L. Lee, D. Ghonasgi, and E. Lomba, J. Chem. Phys. **104**, 8058 (1996)
[40] A. G. Vompe and G. A. Martynov, J. Chem. Phys. **100**, 5249 (1994)
[41] S. J. Singer and D. Chandler, Mol. Phys. **55**, 621 (1985)
[42] O. E. Kiselyov and G. A. Martynov, J. Chem. Phys. **93**, 1942 (1990)
[43] A. B. Schmidt, J. Chem. Phys. **99**, 4225 (1993)
[44] G. Sarkisov, J. Chem. Phys. **114**, 9496 (2001)
[45] N. Jakse and I. Charpentier, Phys. Rev. E **67**, 061203 (2003)
[46] J. M. Bomont, J. Chem. Phys. **119**, 11484 (2003)
[47] D. Levesque and L. Verlet, Phys. Rev. **182**, 307 (1969)
[48] M. Zacharias, T. P. Straatsma, and J. A. McCammon, J. Chem. Phys. **100**, 9025 (1994)
[49] MATLAB, *version 8.50. (R2015a)*, The MathWorks Inc., Natick, Massachusetts, (2015)
[50] G. Rickayzen and A. Augousti, Mol. Phys. **52**, 1355 (1984)
[51] S. L. Carnie, J. Chem. Phys. **74**, 1472 (1981)
[52] T. Fujita and T. Yamamoto, J. Chem. Phys. **147**, 014110 (2017)
[53] M. Misin, M. V. Fedorov, and D. S. Palmer, J. Chem. Phys. **142**, 091105 (2015)
[54] J.-F. Truchon, B. M. Pettitt, and P. Labute, J. Chem. Theor. Comp. **10**, 934 (2014)
[55] D. Roy, N. Blinov, and A. Kovalenko, J. Phys. Chem. B **121**, 9268 (2017)
[56] T. Luchko, N. Blinov, G. C. Limon, K. P. Joyce, and A. Kovalenko, J. Comp. Aid. Mol. Des. **30**, 1115 (2016)
[57] W. Huang, N. Blinov, and A. Kovalenko, J. Phys. Chem. B **119**, 5588 (2015)
[58] M. Misin, D. S. Palmer, and M. V. Fedorov, J. Phys. Chem. B **120**, 5724 (2016)
[59] H. J. C. Berendsen, J. R. Grigera, and T. P. Straatsma, J. Phys. Chem. **91**, 6269 (1987)
[60] R. O. Watts, J. Chem. Phys. **50**, 984 (1969)
[61] J. G. Kirkwood, J. Chem. Phys. **3**, 300 (1935)
[62] J. G. Kirkwood, J. Chem. Phys. **19**, 275 (1936)
[63] F. Hirata, *Molecular Theory of Solvation*, Kluwer Academic Publishers, Dordrecht, (2003)
[64] B. C. Eu and K. Rah, J. Chem. Phys. **111**, 3327 (1999)